The Number of Microbubbles Generated During Cardiopulmonary Bypass Can Be Estimated Using Machine Learning From Suction Flow Rate, Venous Reservoir Level, Perfusion Flow Rate, Hematocrit Level, and Blood Temperature

Satoshi Miyamoto , Zu Soh, *Member, IEEE*, Shigeyuki Okahara , *Member, IEEE*,
Akira Furui , *Member, IEEE*, Taiichi Takasaki, Keijiro Katayama, Shinya Takahashi ,
and Toshio Tsuji , *Member, IEEE*

Abstract—Goal: Microbubbles (MBs) are known to occur within the circuits of cardiopulmonary bypass (CPB) systems, and higher-order dysfunction after cardiac surgery may be caused by MBs as well as atheroma dispersal associated with cannula insertion. As complete MB elimination is not possible, monitoring MB count rates is critical. We propose an online detection system with a neural network-based model to estimate MB count rate using five parameters: suction flow rate, venous reservoir level, perfusion flow rate, hematocrit level, and blood temperature. Methods: Perfusion experiments were performed using an actual CPB circuit, and MB count rates were measured using the five varying parameters. Results: Bland–Altman analysis indicated a high estimation accuracy ($R^2 > 0.95$, $p < 0.001$) with no significant systematic error. In clinical practice, although the inclusion of clinical procedures slightly decreased the estimation accuracy, a high coefficient of determination for 30 clinical cases ($R^2 = 0.8576$) was achieved between measured and estimated MB count rates. Conclusions: Our results highlight the potential of this system to improve patient outcomes and reduce MB-associated complication risk.

Index Terms—Cardiac surgery, cardiopulmonary bypass, microbubbles, neural network, online detection.

Impact Statement— Estimation model of the number of microbubbles delivered from the venous reservoir was constructed based on the CPB operating conditions used in cardiac surgery.

I. INTRODUCTION

MICROBUBBLES (MBs) generated during cardiopulmonary bypass (CPB), which supports circulation in patients undergoing cardiac surgery, have been identified as a crucial cause of cerebral neuropathy [1]. During cardiac surgery, MBs are delivered into the body by CPB, which may lead to complications [2]. The main cause of MB formation during CPB operations is the inflow of air into the venous blood reservoir owing to the venting or bleeding suction maneuvers performed, and the incoming air can be split into MBs of about 40 μm in diameter [3]. The MBs are then divided further into smaller bubbles of 10–20 μm in diameter during the blood delivery process and are delivered to the patient from the venous reservoir [4], [5].

Despite advancements in CPB techniques that have led to decreased mortality rates in cardiac surgeries, the incidence of postoperative cerebral neuropathy is a major concern, particularly in older patients [6]. The etiology of cerebral neuropathy involves multiple factors such as cerebral ischemia due to low blood flow to the brain, inflammatory reactions, and embolisms. In the context of embolisms, MBs are recognized as substantial contributing factors along with atheromas [7].

During cardiac surgery, MBs can be generated by various factors, including aortic manipulation, cannula insertion,

cross-clamping, air introduced into the CPB venous line, vent flow rate, cardiotomy suction, and decreases in the venous blood reservoir level [8], [9], [10], [11], [12], [13], [14], [15]. Additionally, the design of venous reservoirs, high blood flow rates, and high-temperature gradients may contribute to MB formation [16]. MBs, composed of nitrogen-containing gases, do not easily dissolve in the body and can cause capillary occlusion [17]. Specifically, when MBs enter the body, they can obstruct 10-μm capillaries, leading to microemboli and resulting in postoperative brain dysfunction in patients undergoing CPB surgery [18]. Moreover, because of their poor solubility, MBs aggregate in blood vessels and form larger bubbles [19]. These large bubbles can occlude large blood vessels and develop into infarcts [20], [21], [22]. Additionally, when MBs come into contact with venous vessel walls, they can induce inflammation similar to that in arterial walls [23]. Inflammatory reactions in cerebral blood vessels can increase the permeability of vessel walls, leading to cerebral edema and brain dysfunction. Cognitive decline is a common complication following cardiac surgery and affects approximately 26%–40% of patients [24]. Therefore, recent studies have highlighted the importance of preventing the generation of MBs and their entry into a patient's body [24], [25], [26].

Ideally, all MBs should be removed. Therefore, each part of the CPB, including the venous reservoir, membrane oxygenator, and arterial filter, is equipped with MB removal functions. For example, a venous reservoir with a large volume increases the transit time of blood flow and uses the buoyancy of MBs to remove them [27]. Although modern equipment, techniques, and perfusion technologies have reduced the likelihood of massive air embolisms, MBs are still transferred to patients [28]. Therefore, MBs during CPB remain a concern because of postoperative neurological deficits. Consequently, for several years, the generation mechanisms and defoaming techniques of MBs have attracted considerable attention [29], [30], and monitoring the MB count rate during CPB has become critical [31], [32], [33], [34]. The current CPB system is equipped with a noninvasive ultrasonic bubble sensor that can detect and warn about the presence of air bubbles with diameters > 300 μm. Recently, MBs with diameters of larger than 25 μm have been detected with highly accurate ultrasonic sensors [16]; however, owing to the high cost of the devices, they are not yet widely used in general clinical practice. Additionally, the conditions under which MBs increase have not been systematically studied.

The number of MBs delivered to patients during CPB can be reduced by minimizing the number of MBs counted at the outlet of the venous reservoir [35]. In our previous in vitro experiments using bovine blood, four factors were strongly associated with MB generation: cardiotomy suction, venous reservoir level, perfusion flow rate, and blood viscosity [36], [37]. Blood viscosity, however, is influenced by various subfactors including blood temperature, hematocrit (Hct), and blood cell morphology, and the specific contribution of these subfactors to the MB count rate remains still unknown. Moreover, if an online detection model for the number of MBs generated during CPB can be established, we can reduce MB outflow by providing immediate feedback to the operator to change the set conditions of CPB.
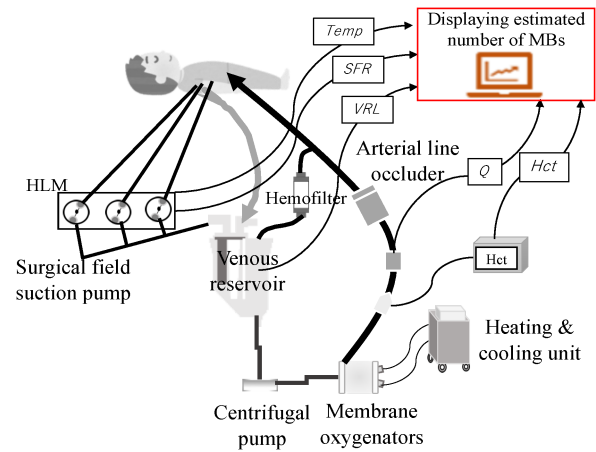

Fig. 1. Overview of the cardiopulmonary bypass circuit and proposed system. The proposed system measures the blood temperature, suction flow rate, venous reservoir level, perfusion flow rate, hematocrit value, and inlet and outlet pressure. HLM: heart-lung machine; SFR: suction flow rate; VRL: venous reservoir level; Q: perfusion flow rate; Hct: hematocrit; Temp: temperature; MBs: microbubbles.

To address these limitations, this study estimated the MB count rate in a venous reservoir, which is the primary source of MB generation. Perfusion experiments were conducted using various blood configurations and CPB parameters. Correlation analysis was performed to determine the contribution of each factor to the MB count rate, including the influence of the sub-factors of blood viscosity, by manipulating blood temperature and Hct value under the condition that blood cell morphology is normal. Then, we developed a novel five-factor feedforward model to assess the accuracy of the MB count rate estimation, and permutation importance was used to evaluate the contribution of each factor. The model constructed using a neural network was obtained from a bovine blood experiment. Therefore, a clinical evaluation was conducted during CPB surgery to evaluate differences between human and bovine blood and to demonstrate clinical applicability.

II. Materials and Methods

A. Proposed System

Fig. 1 shows the proposed MB estimation system incorporated into a CPB. The system comprises a venous blood reservoir, centrifugal pump, membrane oxygenator, arterial filter, hemoconcentrator, and tubes that connect the patient to the CPB. Blood from the patient is stored in a venous blood reservoir through a defoaming and filtering in the cardiotomy reservoir, delivered to the patient through a centrifugal pump, and oxygenated using a membrane oxygenator equipped with an arterial filter to trap particular emboli and MBs. Then, the blood temperature is controlled via a heat exchanger built into the membrane oxygenator using a heating and cooling unit. Finally, the blood is returned to the patient through an arterial line.

The proposed system was connected to the CPB circuit, and the following parameters were measured: blood temperature, cardiotomy suction, flow rate, venous reservoir level, perfusion
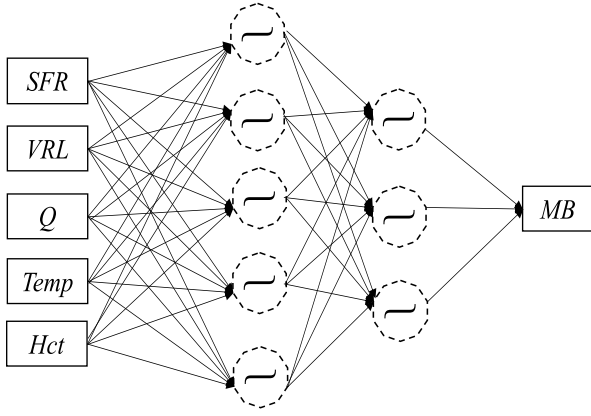
Fig. 2. Neural network model to estimate the microbubble count rate. SFR: suction flow rate; VRL: venous reservoir level; Q: perfusion flow rate; Hct: hematocrit; Temp: temperature; MB: microbubble.

flow rate, and Hct values. Furthermore, using our previous system [36], [37], blood viscosity was estimated in real time using inlet and outlet pressures of the membrane artificial lung and perfusion flow rate. The MB count rate was estimated using measured and estimated parameters. Thus, the proposed system enables monitoring of the MB count rate for any general CPB. The proposed system also incorporates a computer to estimate the MB count rate based on measured CPB parameters (upper-right panel of Fig. 1).

Fig. 2 depicts the proposed two–three-layer neural network-based model for estimating the MB count rate, which is very simple; thus, it can be easily implemented and enables online detection of MB generation. The model includes an input layer, a hidden layer, and an output layer, which are mathematically represented by the following equations:

$$MB = w_{3,0} + \sum_{h=1}^{H} w_{3,h} x_h \tag{1}$$

$$x_h = \tanh\left(w_{2,0} + \sum_{i}^{N} w_{2,h,i} x_i\right) \tag{2}$$

$$x_i = \tanh\left(w_{1,0} + w_{1,i,SFR} SFR + w_{i,VRL} VRL \right.$$
$$\left. + w_{i,Q} Q + w_{i,Hct} Hct + w_{i,Temp} Temp\right) \tag{3}$$

where SFR is the suction pump flow rate; VRL is the reservoir level; Q is the perfusion flow rate; Hct is the hematocrit value; Temp is the blood temperature; $w_{j,0}(j = 1, 2, 3)$ denotes the bias term; and $w_{3,h}, w_{3,h}, w_{2,h,i}, w_{1,h,\xi}$ represent the weight parameters, where the first subscript designates the layer, h and i index the neuron unit; and $\xi \in (SFR, VRL, Q, Hct, Temp)$ corresponds to the input parameter. The unit numbers of the input and hidden layers were determined to be $N = 5$, $H = 3$. To differentiate the proposed model from our previous one, it is referred to as the five-factor input model. In our previous studies [36], [37], we used blood viscosity (V) as the input for the neural network model. This is because blood viscosity affects the buoyancy and ascent velocity of MBs, which in turn influences the residence duration of MBs and ultimately affects the number of MBs
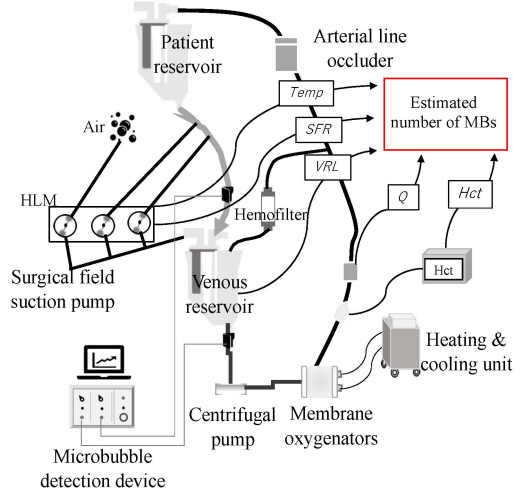

Fig. 3. Experimental circuit. In the experimental setting, the patient was replaced by a patient reservoir. Air was injected into the suction circuit to simulate air introduction from the surgical field. An MB detection device was installed in the CPB circuit to measure the MB count rate. HLM: heart-lung machine; SFR: suction flow rate; VRL: venous reservoir level; Q: perfusion flow rate; Hct: hematocrit; Temp: temperature; MB: microbubble.

delivered to a patient's body. This model is referred to as the four-factor input model, and its input layer is expressed by the following equation instead of the one shown in (3):

$$x_i = \tanh\left(w_{1,0} + w_{1,i,SFR} SFR + w_{1,i,VRL} VRL \right.$$
$$\left. + w_{1,i,Q} Q + w_{1,i,V} V\right) \tag{4}$$

Using the proposed system comprising various measurement devices and the MB count estimation model, we were able to estimate MB counts in clinical practice. To validate the effectiveness of this approach, we conducted tests to assess the estimation accuracy through both a perfusion experiment and in clinical practice.

B. Perfusion Experiment

1) Ethics Statement: This study was approved by the Ethics Committee of Hiroshima University (number: E-2773).

2) System: Fig. 3 shows the configuration of the CPB circuit used in the perfusion experiment. All materials were freshly prepared. A reservoir (CAPIOX Venous Reservoir CX-RR40; Terumo Cardiovascular Systems Corporation, Tokyo, Japan) was used to simulate a patient; thus, it was labeled as the patient reservoir. The venous circuit was connected from the patient's reservoir to a hard-shell venous reservoir (HSVR) (CAPIOX Venous Reservoir CX-RR40, Terumo Cardiovascular Systems Corporation). Blood was circulated using the centrifugal pump (Mera Centrifugal Pump HCF-MP23^{TM}, Senko Medical Instrument, Manufacturing Co Ltd., Tokyo, Japan), oxygenated using a hollow fiber membrane oxygenator (CX-FX15E, Terumo Cardiovascular Systems Corporation), and then returned to the patient reservoir. CX-FX15E has a unique capability to process air bubbles being absorbed through the microporous fibers [38]. The fluid level in the HSVR was controlled using an electric

regulator (HASII-RE, Senko Medical Instrument, Manufacturing Company, Ltd., Tokyo, Japan). A circuit simulating intraoperative blood suction was connected to both the venous circuit and patient reservoir. The flow rate of the aspirated blood was regulated by a roller pump placed between the patient and venous reservoirs. A 6-mm tube was used to simulate air suction in the surgical field, and a roller pump was used to regulate the airflow. The aspirated blood and air passed through a Y-shaped connector, where they were mixed and returned to the HSVR. To adjust the blood volume (Hct value), a hemoconcentrator (Hemocrystal HC11, Senko Medical Instrument, Manufacturing Company, Ltd.) was connected to the outlet of the membrane artificial lung and incorporated back into the HSVR. During the experiment, the circuit connected to the hemoconcentrator was blocked with forceps to prevent blood from recirculating.

The blood reservoir capacity of the HSVR was 4000 mL, and a 40-μm internal screen filter was connected to the reservoir. The removed microaggregates, e.g., blood and fat clots, could be aspirated from the surgical field. The air bubbles were filtered through a polyurethane defoamer. The minimum volume of the HSVR was 150 mL. The membrane oxygenator used in the experiment incorporated a screen mesh filter on the arterial side with a 32-μm pore size attached to the outside of the fiber layer to remove microaggregates, including air bubbles, blood clots, and fat clots. The hollow fibers of the hemoconcentrator were composed of polysulfone. The CPB device was HAS II (Senko Medical Instrument, Inc.); the diameter of the roller pump for suction was $70\,\varphi$. A pulsed ultrasound Doppler device (Model BC-100, GAMPT, Merseburg, Germany) was used to detect MB outflow in the range of 10–250 μm from the HSVR. The measurement accuracy of Model BC-100 is $\pm 10\%$. The probe was attached to the tube using an ultrasonic gel to exclude air. The probe was also mounted under the patient reservoir to prevent air from flowing out.

Sodium citrate was used to preserve fresh whole bovine blood (1000 mL; DARD Co., Ltd., Tokyo, Japan), and heparin was used to prevent blood clots. The activated clotting time was set at 500 s. For the perfusion solution, 700 mL of bovine blood was diluted with 300 mL of lactated Ringer solution to obtain a solution of 1000 mL. Bovine blood was used for in vitro experiments.

3) Protocols: Experiments were performed to determine the relationship between the MB count rate and associated factors. The circuit was primed with a perfusate prepared by mixing 1000 mL of bovine blood and 1000 mL of Ringer acetate solution. The speed of the centrifugal pump was 2500 rpm, and the number of MBs was measured by varying combinations of the following parameters. The arterial flow was adjusted to 4.0, 3.5, 2.5, and 2.0 L/min using an arterial occluder. The HSVR levels in the reservoir were adjusted to 1000, 700, 500, 300, and 200 mL. The suction flow rate was set at 400 mL/min, while air pump flow rates were set at 1.5, 1.3, 1.1, 0.9, 0.7, 0.5, and 0.3 L/min to simulate air suction in the surgical field. The blood temperature was adjusted to 35, 30, 25, and 20 °C. The Hct values were adjusted to 20, 25, 30, and 35% using a hemoconcentrator. T The ranges of the partial pressures of the gas during the experiment were 132–215 mmHg and 25–33.2 mmHg for oxygen and carbon dioxide, respectively, and the range of pH is 7.36–7.55.

Blood gas analysis was performed using blood collected from the outlet of the membrane oxygenator.

Each parameter was set within the normal range implemented in the system at the Hiroshima University Hospital. MBs were initially measured at an Hct value of 20%, and all possible combinations of the reservoir level, suction flow rate, perfusion flow rate, and blood temperature were determined. After each combination of measurements was completed, dehydration was performed to adjust the Hct value. Measurements were performed when the MB count rate was stabilized by changing the experimental parameters. MB measurements were performed at 5-min intervals, and the median value was calculated. During the experiment, CO2 was gasified at 5 L/min around the air suction site to simulate surgical conditions. Carbon dioxide is about 40 times more soluble in liquids than in room air, and to suppress the formation of MBs, room-temperature air was replaced with carbon dioxide gas. The measurement time was 5 min for each condition. The measured MB numbers are presented as median values at 1-s intervals.

4) Analysis: Neural network parameters were trained using the gradient descent method to fit the measured MB values. The parameters of the model were validated using 10-fold cross-validations by randomly dividing the measured data into 10 subsamples of equal size; nine subsamples were used as training data, and the training parameters were validated using the remaining subsample. This procedure was repeated 10 times with different combinations of training and validation data. The estimation accuracies of the models were assessed using the coefficient of determination between the estimated and measured MB count rates and the Bland–Altman plot.

The root means square error (RMSE) values between the estimated and measured values for the same viscosity, but different Hct values and blood temperatures were compared using Student's t-test. Statistical significance was set at p values <0.05. (See Supplementary Materials for more information) Finally, permutation importance analysis [39] was conducted on the trained five-factor model to assess the contributions of the input factors. (see Supplementary Material for the proof). This analysis evaluates the importance of the input factor by randomly permutating the observation values of the target factor. Then, the increase in RMSE between the estimated and measured values resulting from this random permutation can be interpreted as an index for assessing the importance of the permutated factor. In this analysis, the average RMSE was obtained using a 10-fold cross-validation method. All the aforementioned data analyses were performed using JMP14 (SAS Institute Inc., Cary, NC, USA).

C. Clinical Experiment

1) Ethics Statements: The Ethical Review Committee approved all epidemiological research experiments at Hiroshima University (number: E-2773), and informed consent was obtained from all patients. The study was conducted in accordance with the principles of the Declaration of Helsinki.

2) Methods: To evaluate differences between human and bovine blood and demonstrate clinical applicability of the estimation model, a clinical evaluation was performed on 30
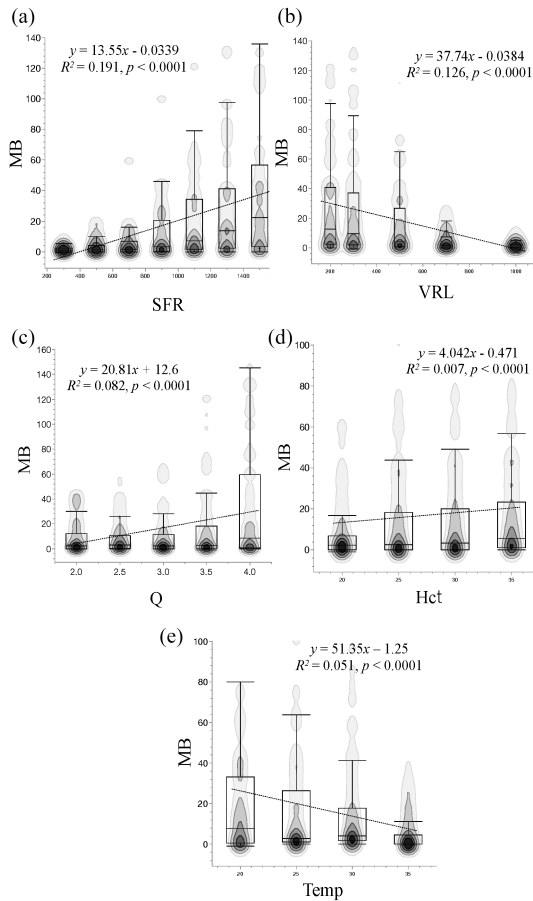
Fig. 4. Correlation between each factor and the MB count rate. Plots (a), (b), (c), (d), and (e) show the MB count rate as a function of the suction flow rate, venous reservoir level, perfusion flow rate, hematocrit value, and blood temperature, respectively. The dotted lines denote linear regression approximations. MB: microbubble; SFR: suction flow rate; VRL: venous reservoir level; Q: perfusion flow rate; Hct: hematocrit; Temp: temperature.

TABLE I
PARTIAL CORRELATION COEFFICIENTS OF FACTORS ASSOCIATED WITH THE MB COUNT RATE

	VRL	SFR	Q	Temp.	Hct	MB
VRL	1	0.2323	0.1665	0.2137	0.0819	−0.4978***
SFR	0.2323	1	−0.1915	−0.2458	0.0848	0.5889***
Q	0.1665	−0.1915	1	−0.1232	0.1098	0.4336***
Temp.	0.2137	−0.2458	−0.1232	1	0.1118	−0.4725***
Hct	0.0819	0.0848	0.1098	0.1118	1	0.3258***
MB	−0.4978***	0.5889***	0.4336***	−0.4725***	0.3258**	1

VRL: venous reservoir level, SFR: suction flow rate , Q: perfusion flow rate, Temp.: blood temperature, Hct: hematocrit value, MB: microbubble count rate. ***: $p < 0.001$
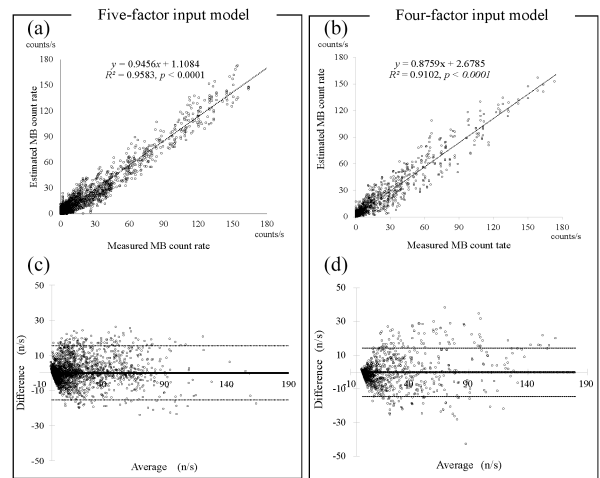

Fig. 5. Estimation accuracies of the MB count rate. (a) shows the MB count rates estimated using the five-factor input model proposed in this study, and (b) shows that estimated using the previously proposed four-factor input model. (c) and (d) show the Bland–Altmann plot for (a) and (b), respectively. The solid line denotes the bias (mean of the difference), the large dashed line denotes the 95% limits of agreement (two standard deviations of difference), and the small dashed lines denote the 95% confidence interval for the difference.

patients who underwent cardiac surgery with CPB. During surgery, the suction and vent flow rates were adjusted to maintain perfusion flow at a confidence interval of approximately 2.5 L/min/m². The blood delivery temperature was controlled between 32 °C and 34 °C. Hct values ranged between 21% and 30%. Blood cardioplegia was administered between 5 °C and 15 °C at 20-min intervals, and a 36 °C hotshot was administered before declanp. All data were measured using the same system shown in Fig. 3 with the Model BC-100 MB measuring device installed at the outlet of the venous reservoir.

III. RESULTS

A. In Vitro Experiment

Correlation analysis was conducted between the five factors and MB count rate by performing perfusion experiments using bovine blood. Fig. 4 plots the MB count rate against each factor, and Table I shows the partial correlations. These analyses revealed no significant partial correlations between any pair of factors. However, moderate partial correlations were observed

between the MB count rate and five factors ($0.3 < |r| \leq 0.6, p < 0.001$).

The MB count rate estimated using the five-factor input model demonstrated high estimation accuracy ($R^2 = 0.9583, p < 0.001$) (Fig. 5(a)). The MB count rate estimated using the four-factor input model through 10-fold cross-validation indicated high estimation accuracy ($R^2 = 0.9102, p < 0.001$) (Fig. 5(b)). The analysis results for the five-factor-input model exhibited a mean bias of −0.06, standard deviation of 7.35, limit of agreement (LOA) ranging from −14.53 to 14.29, and percentage error of 11.9%, indicating no significant fixed or proportional bias ($R^2 = 0.1674, p > 0.05$) (Fig. 5(c)). The analysis results for the four-factor input model exhibited a mean bias of 0.20, standard deviation of 7.24, LOA ranging from −13.98 to 14.39, and percentage error of 11.7%, indicating that no significant fixed and proportional bias ($R^2 = 0.1921, p > 0.05$) (Fig. 5(d)).
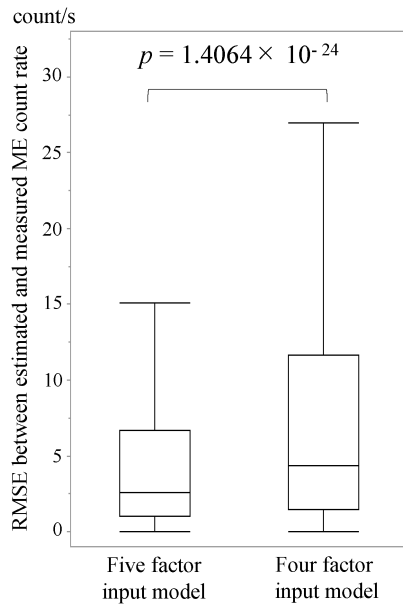
Fig. 6. Estimation error of the MB count rate. The left and right boxplots present the estimation error of the five-factor and four-factor input models, respectively. The vertical axis is the RMSE between the measured and estimated MB count rates in counts per second (count/s). The boxplots are presented with 2.5%, 50% (median), and 97.5% quantile and whiskers for the minimum and maximum values. MB: microbubble; RMSE: root mean square error.
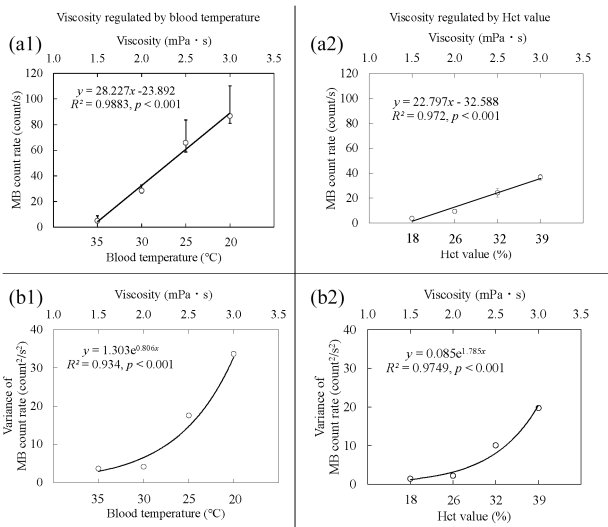

Fig. 7. Relationship of the mean and variance of MB count rates with blood temperature and Hct value. (a1) and (a2) show the mean MB count rates in counts per second [count/s], and (b1) and (b2) show the variances of MB count rates. The left and right graphs show the blood viscosity adjusted by the temperature and Hct value, respectively. MB: microbubble; Hct: hematocrit.

Fig. 6 shows the estimation errors of the five- and four-factor input models. Student's t-test indicated a significant difference between the estimation errors ($p < 0.001$), revealing that the five-factor input model yielded better estimation accuracy than the four-factor input model.
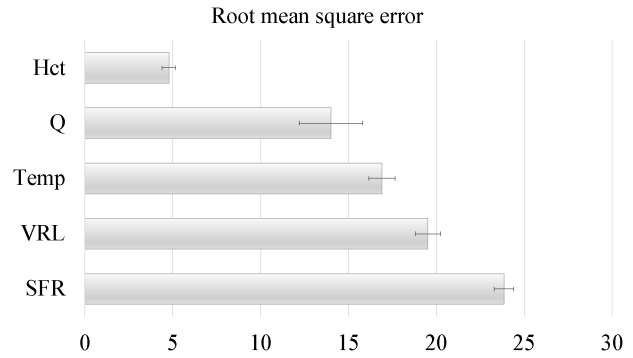

Fig. 8. Root means square error. The horizontal axis shows the root mean square error between the measured and estimated MB counts rate. Hct: hematocrit; Q: perfusion flow rate; Temp: temperature; VRL: venous reservoir level, SFR: surgical field suction.

TABLE II
PATIENT CHARACTERISTICS

Disease	MVR:23 CABG:2 AVR:5
Sex (men: women)	18:12
Age (years)	76 ± 5.4
Body surface area (m^2)	1.61 ± 0.16
ECC (min)	198.1 ± 62.2
ACC (min)	151.5 ± 25.5
Body temperature (°C)	34.3 ± 2.1 (32–36)

MVR: mitral valvuloplasty, CABG: coronary artery bypass grafting, AVR: aortic valve replacement, ECC: extracorporeal circulation time, ACC: aortic cross-clamp time. Data are presented as ratio, mean±standard deviation, or range.

Fig. 7(a1) and (a2) show the mean MB count rates in the outflow from the venous reservoir, indicating that they increased with the blood temperature and Hct values. High linear regression values, where $R^2 = 0.9883$ for temperature and $R^2 = 0.972$ for the Hct value, indicated proportional linear relationships between the MB count rate and temperature and Hct values. The variance of the MB count rate also increased with the temperature and Hct value, but their relationships were nonlinear, and the use of exponential functions accounts for their relationships ($R^2 > 0.93$, $p < 0.001$).

Fig. 8 shows the importance of the input factors. When random permutations were performed for each input, the RMSEs of the suction flow rate, venous reservoir volume, blood temperature, perfusion flow rate, and Hct value increased by approximately 23.8%, 19.5%, 16.9%, 14.0%, and 4.7%, respectively.

B. Clinical Experiment

A clinical experiment was performed in 30 patients who underwent cardiac surgery with cardiopulmonary bypass (Table II).

Fig. 9(a) plots the measured and estimated values excluding MB data points increased by procedures performed by the operator, including transfusion, blood transfusion, and drug administration, with a coefficient of determination $R^2 = 0.8576$ ($p < 0.001$). The corresponding Bland–Altman analysis plot
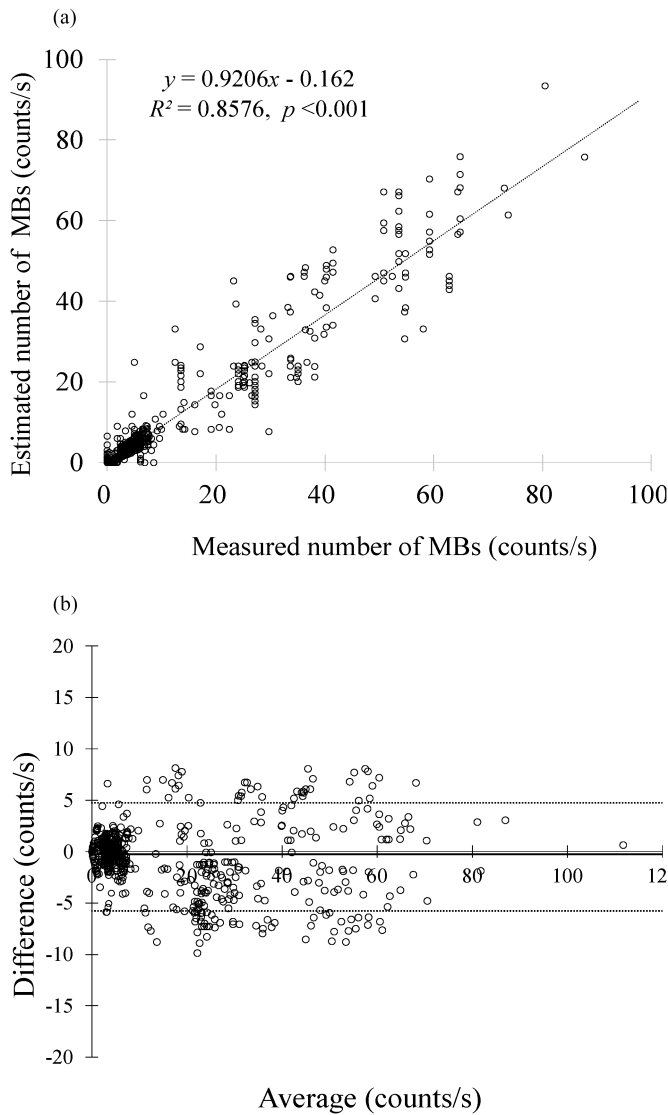
(a)

(b)

Fig. 9. Prediction accuracy of the proposed model. Scatter plot and bland-altman analysis between the estimated and measured numbers of MBs throughout the surgery duration. Correlation and linear regression analyses of the equation to estimate microbubble value and microbubble measurement with a BC-100 microbubble counter are shown in (a). The bland–altmann plot is shown in (b). The solid lines denote the bias (mean of the difference), the thick dashed lines denote the 95% limits of agreement, and the small dashed lines denote the 95% confidence interval for the difference.

showed a mean bias of 0.04, a standard deviation of 1.48, an LOA of -4.56 to 4.74, and an error of 5.3%. These results indicated no significant fixed and proportional biases ($R^2 = 0.2749$, $p > 0.05$), showing no systematic error Fig. 9(b). The treatments were defined as procedures in which perfusionist performed rapid infusion or transfusion of blood into a venous reservoir during cardiopulmonary bypass.

IV. DISCUSSION

Various complications result from CPB, which can be life-threatening [40]. Embolism caused by MBs results in brain dysfunction and cognitive decline [41]. Although the size and number of MBs associated with cognitive decline are debated, emboli have been linked to such clinical outcomes [30], [40]. Previous studies have suggested that MBs should be removed from venous reservoirs to reduce their number after arterial filtering [35]. Therefore, we constructed a model that estimates the MB count rate from rate five measurable factor using a general CPB circuit.

Correlation analysis indicated that the blood temperature and venous reservoir level were negatively correlated with the MB count rate (Fig. 4). This is because as the blood temperature decreases, the velocity of MBs suspended in the venous reservoir increases, thus decreasing the MBs delivered from the venous reservoir. A higher venous reservoir level renders the location of MB generation farther away from the outlet of the venous reservoir and decreases MB retraction through the negative pressure of the centrifugal pump. The Hct value, blood perfusion rate, and surgical suction flow rate were positively correlated with the MB count rate (Fig. 4) because as the Hct value increases the blood viscosity, the velocities of MBs floating in the venous reservoir decrease, thereby increasing the MB count rate. At the venous reservoir outlet, the blood perfusion rate generates a negative pressure; therefore, the number of MBs delivered increases with the flow rate. Notably, cardiotomy suction increases both the MB generation and count rate because it draws air into the venous reservoir. Considering these factors in the neural network-based model enabled an accurate estimation of the MB count rate for both the four- and five-factor input models.

To analyze the impact of each factor on the model, the importance of each input factor was assessed using the permutation importance method [41]. The results showed that a random permutation of the blood temperature increased the RMSE by 16.8 points, whereas that of the Hct value increased by 4.8 points, indicating that blood temperature is crucial in determining the MB count rate.

Further analysis demonstrated an exponential relationship between blood viscosity and variance in MB count rates. It should be noted that the increasing rates of the MB count variances differed depending on factors, blood temperature and Hct value, used to regulate viscosity. These results suggest that changes in blood viscosity due to changes in blood temperature and Hct value may affect the behavior of MBs. Previous studies using water reported decreases in the increasing rate of MBs in a liquid with increasing viscosity and deformations in MBs [42]. MBs, in distilled water at 20 °C, rise at a rate of 20 cm/h, faster than nanobubbles that rise at 1.9 cm/h [43]. MBs in liquids, including blood, contain various electrolytes, plasma, and blood cell components, which may enhance the influence of the surrounding particles. Because the diffusion velocities of MBs are related to their density, an increase in the fluid density due to temperature changes may result in a decrease in the diffusion velocity. Plasma is the primary component of blood, and a decrease in temperature increases its viscosity and obstructs its flow. Compared with the effect of molecules, the effect of external factors, including plasma components, on MBs is more significant and may reduce diffusion velocity. Considering the behavior of MBs in distilled water, an increase in blood viscosity should decrease the movement of MBs and increase the number

of outflows. In contrast, the Hct value increased the viscosity of the blood owing to an increase in the number of red blood cells. In this case, the plasma was unaffected, allowing MBs to pass through the blood cells. Therefore, the number of delivered MBs did not increase significantly.

An accurate estimation of the MB count rate may enable monitoring of the rate in general CPB. Therefore, incorporation of this estimation system may partially prevent embolism-related complications. However, the model parameters were trained based on materials used in the experiments; thus, the MB count rates may vary when using different venous blood reservoirs or centrifugal pumps. Additionally, because blood temperature affects plasma, the viscosities of bovine and human blood may differ due to the reaction of plasma proteins. Herein, the MB count rate differed depending on factors used to regulate the viscosity of the same blood sample, suggesting that changes in blood cell morphology that affect blood viscosity also affect the MB count rate. These issues should be addressed in future studies.

This study had limitations. We could not examine whether a change in partial pressure of blood oxygen affects the MB outflow. This study presents a model to estimate the number of MBs delivered through the venous reservoir outlet. The measurements were conducted at the venous reservoir outlet, which is where the highest concentration of MBs are delivered in artificial cardiopulmonary bypass systems. However, measurements of MBs delivered to the patient were not obtained. In the future, it is necessary to investigate the relationship between the number of MBs delivered from the venous reservoir and the number of MBs delivered to the patient. Additionally, the safe range of the number of MBs delivered from the venous reservoir has not been studied. It was difficult to incorporate methods, including infusion into the model, because they are not performed under certain conditions. Therefore, the time of transfusion or blood transfusion was excluded from the clinical evaluation. The surgical deairing technique after endocardial procedures may produce MBs that can cause cerebral infarction.

V. CONCLUSION

We developed a simple online detection model for MBs during CPB and applied it to surgical cases. The experimental results showed that there was no systematic error in the estimation model in any case. These findings are promising; however, further research involving a larger sample size and diverse surgical scenarios is warranted to validate and generalize these findings.

CONFLICT OF INTEREST

The authors declare that the research was conducted in the absence of any commercial or financial relationships that could be construed as a potential conflict of interest.

AUTHOR CONTRIBUTIONS

S. M. wrote the initial draft, and Z. S. and T. T. edited the manuscript. S. M. and T. T. performed the experiments. S. M. and S. O. measured the data and analyzed the results. Z. S.

contributed to data interpretation. S. O., A. F., T. T., K. K., and S. T. provided critical feedback and helped shape the research, analysis, and manuscript. All authors reviewed the manuscript.

REFERENCES

[1] M. F. Newman et al., "Central nervous system injury associated with cardiac surgery," *Lancet*, vol. 368, no. 9536, pp. 694–703, 2006.

[2] L. Gao, R. Taha, D. Gauvin, L. B. Othmen, Y. Wang, and G. Blaise, "Postoperative cognitive dysfunction after cardiac surgery," *Chest*, vol. 128, no. 5, pp. 3664–3670, 2005.

[3] C. M. Muth and E. S. Shank, "Gas embolism," *New England J. Med.*, vol. 342, no. 7, pp. 476–482, 2000.

[4] G. J. Myers, C. Voorhees, R. Haynes, and B. Eke, "Post-arterial filter gaseous microemboli activity of five integral cardiotomy reservoirs during venting: An in vitro study," *J. Extra-Corporeal Technol.*, vol. 41, no. 1, pp. 20–27, 2009.

[5] J. C. Bird, R. de Ruiter, L. Courbin, and H. A. Stone, "Daughter bubble cascades produced by folding of ruptured thin films," *Nature*, vol. 465, no. 7299, pp. 759–762, 2010.

[6] D. T. Dinh et al., "Trends in coronary artery bypass graft surgery in Victoria, 2001-2006: Findings from the australasian society of cardiac and thoracic surgeons database project," *Med. J. Aust.*, vol. 188, no. 4, pp. 214–217, 2008.

[7] W. R. Brown et al., "Longer duration of cardiopulmonary bypass is associated with greater numbers of cerebral microemboli," *Stroke*, vol. 31, no. 3, pp. 707–713, 2000.

[8] S. J. Lee and S. Kim, "Simultaneous measurement of size and velocity of microbubbles moving in an opaque tube using an X-ray particle tracking velocimetry technique," *Exp. Fluids*, vol. 39, no. 3, pp. 492–497, 2005.

[9] J. R. Grace, "Shapes and velocities of bubbles rising in infinite liquids," *Trans. Inst. Chem. Eng.*, vol. 51, 1973, Art. no. 116.

[10] S. Okahara et al., "Hydrodynamic characteristics of a membrane oxygenator: Modeling of pressure-flow characteristics and their influence on apparent viscosity," *Perfusion*, vol. 30, no. 6, pp. 478–483, 2015.

[11] S. Okahara et al., "Continuous blood viscosity monitoring system for cardiopulmonary bypass applications," *IEEE Trans. Biomed. Eng.*, vol. 64, no. 7, pp. 1503–1512, Jul. 2017.

[12] T. O. Alexandros et al., "A new wrinkle on liquid sheets: Turning the mechanism of viscous bubble collapse upside down," *Science*, vol. 7, pp. 685–688, 2020.

[13] F. D. Rubens et al., "The cardiotomy trial: A randomized, double-blind study to assess the effect of processing of shed blood during cardiopulmonary bypass on transfusion and neurocognitive function," *Circulation*, vol. 116, no. 11, pp. I89–I97, 2007.

[14] H. K. Chang et al., "Hydrodynamic features of pulmonary air embolism: A model study," *J. Appl. Physiol.: Respir., Environ. Exercise Physiol.*, vol. 51, no. 4, pp. 1002–1008, 1981.

[15] A. K. Kaza et al., "Elimination of fat microemboli during cardiopulmonary bypass," *Ann. Thoracic Surg.*, vol. 75, no. 2, pp. 555–559, 2003.

[16] T. Segers et al., "Optical verification and in-vitro characterization of two commercially available acoustic bubble counters for cardiopulmonary bypass systems," *Perfusion*, vol. 33, no. 1, pp. 16–24, 2018.

[17] E. Stride and N. Saffari, "Microbubble ultrasound contrast agents: A review," *Proc. Inst. Mech. Engineers. Part H*, vol. 217, no. 6, pp. 429–447, 2003.

[18] D. van Dijk et al., "Cognitive and cardiac outcomes 5 years after off-pump vs on-pump coronary artery bypass graft surgery," *JAMA*, vol. 297, no. 7, pp. 701–708, 2007.

[19] N. Bremond et al., "Decompressing emulsion droplets favors coalescence," *Phys. Rev. Lett.*, vol. 100, no. 2, 2008, Art. no. 024501.

[20] J. W. Hammon et al., "Risk factors and solutions for the development of neurobehavioral changes after coronary artery bypass grafting," *Ann. Thoracic Surg.*, vol. 63, no. 6, pp. 1613–1618, 1997.

[21] R. C. Groom et al., "Detection and elimination of microemboli related to cardiopulmonary bypass," *Circulation. Cardiovasc. Qual. Outcomes*, vol. 2, no. 3, pp. 191–198, 2009.

[22] T. Gerriets et al., "Protecting the brain from gaseous and solid microemboli during coronary artery bypass grafting: A randomized controlled trial," *Eur. Heart J.*, vol. 31, no. 3, pp. 360–368, 2010.

[23] M. Barak and Y. Katz, "Microbubbles: Pathophysiology and clinical implications," *Chest*, vol. 128, no. 4, pp. 2918–2932, 2005.

[24] K. K. Martin et al., "Intraoperative cerebral high-intensity transient signals and postoperative cognitive function: A systematic review," *Amer. J. Surg.*, vol. 197, no. 1, pp. 55–63, 2009.

[25] S. Mitchell and D. Gorman, "The pathophysiology of cerebral arterial gas embolism," *J. Extra-Corporeal Technol.*, vol. 34, no. 1, pp. 18–23, 2002.

[26] S. Doganci et al., "Impact of the intensity of microemboli on neurocognitive outcome following cardiopulmonary bypass," *Perfusion*, vol. 28, no. 3, pp. 256–262, 2013.

[27] F. Born et al., "Microbubble activity during extra corporeal life support," *Thoracic Cardiovasc. Surgeon*, vol. 65, no. S01, pp. S1–S110, 2017.

[28] Y. Abu-Omar et al., "Solid and gaseous cerebral microembolization during off-pump, on-pump, and open cardiac surgery procedures," *J. Thoracic Cardiovasc. Surgeon*, vol. 127, no. 6, pp. 1759–1765, 2004.

[29] D. P. Herbst, "Effects of purge-flow rate on microbubble capture in radial arterial-line filters," *J. Extra-Corporeal Technol.*, vol. 48, no. 3, pp. 105–112, 2016.

[30] G. R. DeFoe et al., "Embolic activity during in vivo cardiopulmonary bypass," *J. Extra-Corporeal Technol.*, vol. 46, no. 2, pp. 150–156, 2014.

[31] S. Wagner et al., "Observation of microbubbles during standard dialysis treatments," *Clin. Kidney J.*, vol. 8, no. 4, pp. 400–404, 2015.

[32] A. T. Oratis et al., "A new wrinkle on liquid sheets: Turning the mechanism of viscous bubble collapse upside down," *Science*, vol. 369, no. 6504, pp. 685–688, 2020.

[33] R. A. Rodriguez et al., "Effect of perfusionist technique on cerebral embolization during cardiopulmonary bypass," *Perfusion*, vol. 20, no. 1, pp. 3–10, 2005.

[34] J. E. Souders et al., "Spatial distribution of venous gas emboli in the lungs," *J. Appl. Physiol.*, vol. 87, no. 5, pp. 1937–1947, 1999.

[35] J. Jin et al., "Dynamic tracking of bulk nanobubbles from microbubbles shrinkage to collapse," *Colloids Surfaces A: Physicochemical Eng. Aspects*, vol. 589, 2020, Art. no. 124430.

[36] S. Miyamoto et al., "Neural network-based modeling of the number of microbubbles generated with four circulation factors in cardiopulmonary bypass," *Sci. Rep.*, vol. 11, no. 1, 2021, Art. no. 549.

[37] S. Miyamoto et al., "Neural network-based estimation of microbubbles generated in cardiopulmonary bypass circuit: A clinical application study," in *Proc. IEEE 44th Annu. Int. Conf. Eng. Med. Biol. Soc.*, 2022, pp. 617–620.

[38] S. Bronson, J. B. Riley, J. P. Blessing, M. H. Ereth, and J. A. Dearani, "Prescriptive patient extracorporeal circuit and oxygenator sizing reduces hemodilution and allogeneic blood product transfusion during adult cardiac surgery," *J. Extra-Corporeal Technol.*, vol. 45, no. 3, pp. 167–172, 2013.

[39] A. Altmann et al., "Permutation importance: A corrected feature importance measure," *Bioinformatics*, vol. 26, no. 10, pp. 1340–1347, 2010.

[40] D. E. Haines et al., "Microembolism and catheter ablation II: Effects of cerebral microemboli injection in a canine model," *Circulation. Arrhythmia Electrophysiol.*, vol. 6, no. 1, pp. 23–30, 2013.

[41] P. Hou et al., "Estimate ecotoxicity characterization factors for chemicals in life cycle assessment using machine learning models," *Environ. Int.*, vol. 135, 2020, Art. no. 105393.

[42] S. S. Shapiro and M. B. Wilk, "An analysis of variance test for normality (complete samples)," *Biometrika*, vol. 52, no. 3–4, pp. 591–611, 1965.

[43] M. Takahashi, "ζ potential of microbubbles in aqueous solutions: Electrical properties of the gas-water interface," *J. Phys. Chem. B*, vol. 109, no. 46, pp. 21858–21864, 2005.